Predicting Model of Biochemical Recurrence of Prostate Carcinoma (PCa-BCR) Using MR Perfusion-Weighted Imaging-Based Radiomics

Peng An, MD[1,2] (iD), Yong Lin, MD[3,4], Yan Hu, MD[2,5,3], Ping Qin, MD[3],
YingJian Ye, PhD[2,4] (iD), Weiping Gu, PhD[2,3], Xiumei Li, MD[1,4],
Ping Song, PhD[1,5] (iD), and Guoyan Feng, PhD[1,2]

Abstract

Objective: To build a combined model that integrates clinical data, contrast-enhanced ultrasound, and magnetic resonance perfusion-weighted imaging-based radiomics for predicting the possibility of biochemical recurrence of prostate carcinoma and develop a nomogram tool. **Method:** We retrospectively analyzed the clinical, ultrasound, and magnetic resonance imaging data of 206 patients pathologically confirmed with prostate carcinoma and receiving radical prostatectomy at Xiangyang No. 1 People's Hospital from February 2015 to August 2021. Based on one to 7 years of follow-up (prostate specific antigen [PSA] level≥0.2 ng/mL, indicative of prostate carcinoma–biochemical recurrence), the patients were divided into biochemical recurrence group (n = 77) and normal group (n = 129). The training and testing sets were formed by dividing the patients at a 7:3 ratio. In training set, The magnetic resonance perfusion-weighted imaging–based radiomics radscore was generated using lasso regression. Several predictive models were built based on the patients' clinical imaging data. The predictive efficacy (area under the curve) of these models was compared using the MedCalc software. The decision curve analysis was conducted using the R to compare the net benefit. Finally, an external validation was carried out on the testing set, and the nomogram tool was developed for predicting prostate carcinoma–biochemical recurrence. **Result:** The univariate analysis confirmed that Tumor diameter, tumor node metastasis classification stage of tumor, lymph node metastasis or distance metastasis, Gleason grade, preoperative PSA, ultrasound (peak intensity, arrival time, and elastography grade), and magnetic resonance imaging-radscore1/2 were predictors of prostate carcinoma–biochemical recurrence. On the training set, the combined model based on the above factors had the highest predictive efficacy for prostate carcinoma–biochemical recurrence (area under the curve: 0.91; odds ratio 0.02, 95% confidence interval: 0.85-0.95). The predictive performance of the combined model was significantly higher than that of the model based on general clinical data (area under the curve: 0.74; odds ratio 0.04, 95% confidence interval: 0.67-0.81, P < .05), contrast-enhanced ultrasound (area under the curve: 0.61; odds ratio 0.05 95% confidence interval: 0.53-0.69, P < .05), and the magnetic resonance imaging–based radiomics model (area under the curve: 0.85; odds ratio 0.03, 95% confidence interval: 0.78-0.91, P = .01). The decision curve analysis also indicated the maximum net benefit derived from the combined model, which agreed with the validation results on the testing set. The nomogram tool developed based on the combined model achieved a good performance in clinical applications. **Conclusion:** The magnetic resonance imaging texture parameters extracted by magnetic resonance perfusion-weighted imaging Lasso regression could help increase the accuracy of the predictive

[1] Department of Radiology, Xiangyang No. 1 People's Hospital, Hubei University of Medicine, Xiangyang, China
[2] Department of Urology, Xiangyang No. 1 People's Hospital, Hubei University of Medicine, Xiangyang, China
[3] Department of Gynaecology and Reproductive medicine, Xiangyang No. 1 People's Hospital, Hubei University of Medicine, Xiangyang, China
[4] Department of internal medicine, Xiangyang No. 1 People's Hospital, Hubei University of Medicine, Xiangyang, China
[5] Department of Pharmacy and Laboratory, Xiangyang No. 1 People's Hospital, Hubei University of Medicine, Xiangyang, China

*Peng An, Yong Lin, and Yan Hu contributed equally to this work.

Corresponding Author:
Guoyan Feng, Department of Radiology, Xiangyang No. 1 People's Hospital, Hubei University of Medicine, Xiangyang, China.
Email: fengguoyan2022@yeah.net Ping Song, Department of Pharmacy and Laboratory, Xiangyang No. 1 People's Hospital, Hubei University of Medicine, Xiangyang, China
Email: songping2012@126.com

model. The combined model and the nomogram tool provide support for the clinical screening of the populations at a risk for biochemical recurrence.

Introduction

In Europe, prostate carcinoma (PCa) is one of the most common malignancies in the department of urology. About 400 thousand males are dead with PCa in Europe–US every year.[1,2] In the United States, the incidence of PCa-BCR has surpassed that of lung carcinoma to become the most common carcinoma in males. In recent years, unclean diet, psychological problems, and environmental pollution go together with China's rapid economic development. The incidence (about 9.92 per ten thousand) and mortality (about 30%) of PCa have been increasing every year in China. Radical prostatectomy is a primary treatment for PCa, though the incidence of postoperative biochemical recurrent (BCR) remains high. BCR usually implies the presence of residual PCa lesion after the surgery. It has been reported that early prediction and treatment of BCR after surgery can improve the survival rate of PCa.[3] At present, nearly all single predictors of PCa-BCR have certain limitations. In China, PCa patients are generally 65+ years old. Due to patients' lack of medical knowledge, insensitivity to prostate specific antigen (PSA) reagents, and insufficient interpretation of PCa guidelines, many patients or even doctors mistakenly believe that the prognosis of PCa is as good as that of papillary thyroid carcinoma. The comprehensive monitoring and follow-up of PCa can be hardly put into clinical practice in China. Choosing the target population for BCR screening is of high importance for further treatment.[4,5] It has been reported that tumor node metastasis classification (TNM) staging, preoperative PSA, and Gleason grade are risk factors for BCR in PCa. Murat *et al*[6] believed that the probability of BCR was >50% at 24 to 48 months postoperatively when the patients have combined 3 or more risk factors. But according to Consensus of Chinese experts on PCa, the false positive rate using this prediction method reached 16% to 32%.[6–8] Magnetic resonance imaging (MRI) is an ideal method for PCa because of its high tissue resolution and multidirectional sectional imaging; Perfusion-weighted imaging (PWI) shows the blood perfusion at the level of tissue capillaries through magnetic resonance imaging, which can quickly, accurately, and almost noninvasively evaluate the hemodynamic changes in microvessels. The occurrence, development, invasion, and metastasis of tumors at different stages depend on the formation of tumor neovascularization. Assessing the tumor blood perfusion level is of great significance for understanding the biological behavior and prognosis of tumors. Therefore, magnetic resonance perfusion-weighted imaging (MR-PWI) has important clinical value in this study. To reduce biases, we used preoperative MR-PWI sequences for radiomics parameter screening based on lasso regression. A combined model was built by integrating radiomics features and clinical and contrast-enhanced ultrasound (CEUS) data to achieve a good benefit. Our study throws some new light on PCa-BCR prediction. We reviewed literature reports on PCa published in the past 40 years. The existing studies are generally focused on the treatment method and the molecular basis of PCa (Figure 1). Few have discussed the clinical-ultrasound-MRI-PWI combined model for predicting PCa-BCR.[8–10]

Materials and Method

Patients

We retrospectively randomly analyzed the clinical and radiographic data of 245 patients pathologically confirmed with PCa at Xiangyang No. 1 People's hospital from February 2015 to August 2021. The patients were aged 42.3 to 102.1 years old, with an average of 68.26 ± 10.84. Inclusion criteria: (1) The patients conformed to the diagnostic criteria for PCa as per the American Urological Association Guidelines[9,11]; (2) Only single lesions not combined with metastases and visible on MRI and ultrasound were studied to reduce biases; (3) The patients had treatment-naive primary PCa and no history of other carcinomas; and (4) The patients had complete clinical and radiographic data and good compliance and had received
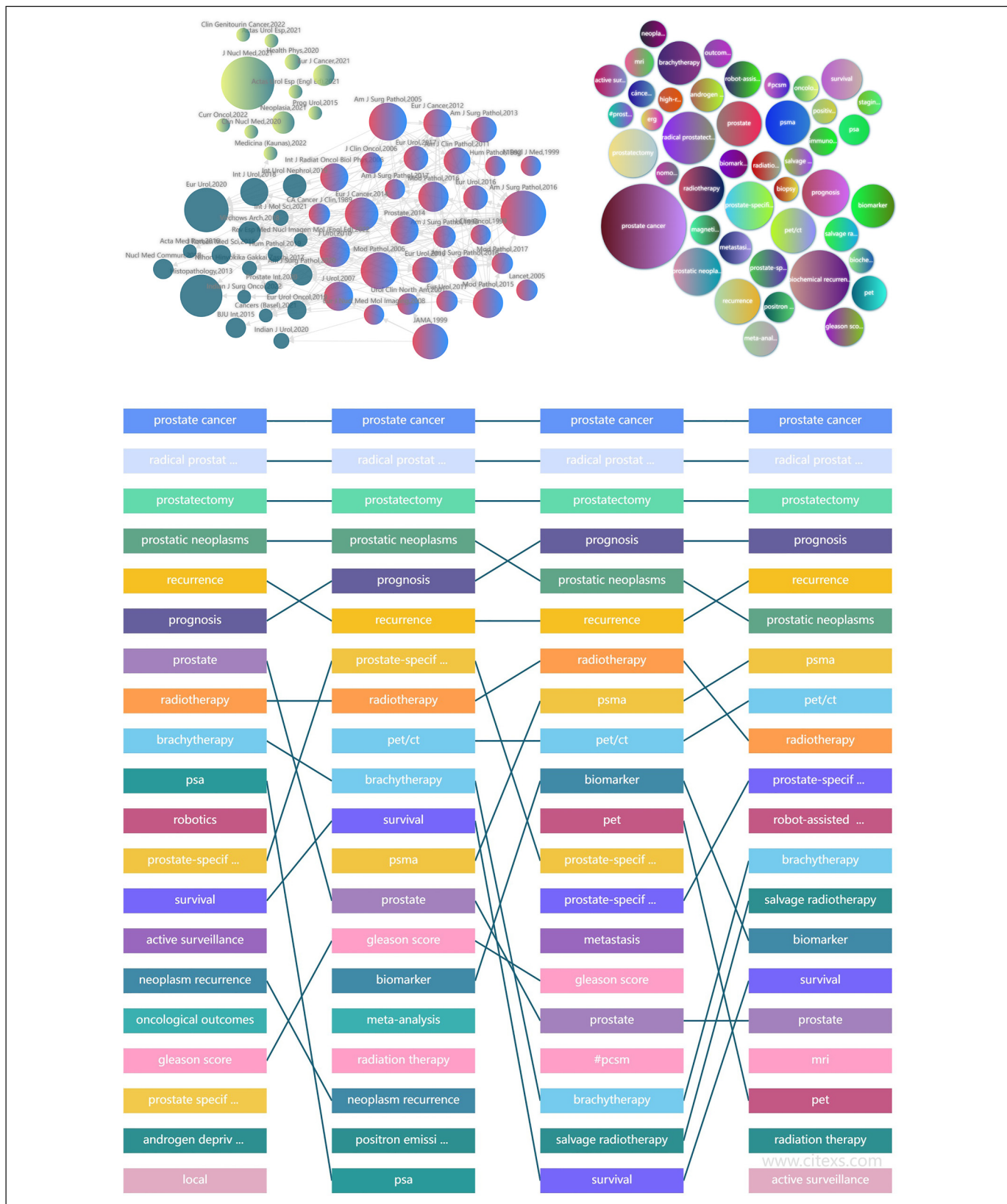
Figure 1. From the content of references retrieval from 1982 to 2022, biochemical recurrence (BCR) has always been a research hotspot, with more research on molecular mechanism and BCR management and less on prediction of BCR by multimodal radiomics. Novelty of the work is a prediction model/nomograph tool established using the multimodal radiomics (MRI-PWI) combined with clinical data ultrasound, which has not been reported before. The specific method to obtain the figure: log in to https://www.citexs.com/ website, select "AI literature big data analysis," enter "BCR," adjust the time node to "1982–2022," and then confirm to "export the figure."

Figure 2. The simplified inclusion and exclusion criteria for pca patient enrollment in the present study.

long-term follow-up. Exclusion criteria: (1) Patients with other carcinomas; (2) patients with contraindications to CEUS/MRI, including congenital heart diseases, heart failure, liver and kidney dysfunction, or drug allergy; (3) patients with cognitive dysfunction; and (4) patients dead for other reasons (Figure 2).[10,11]

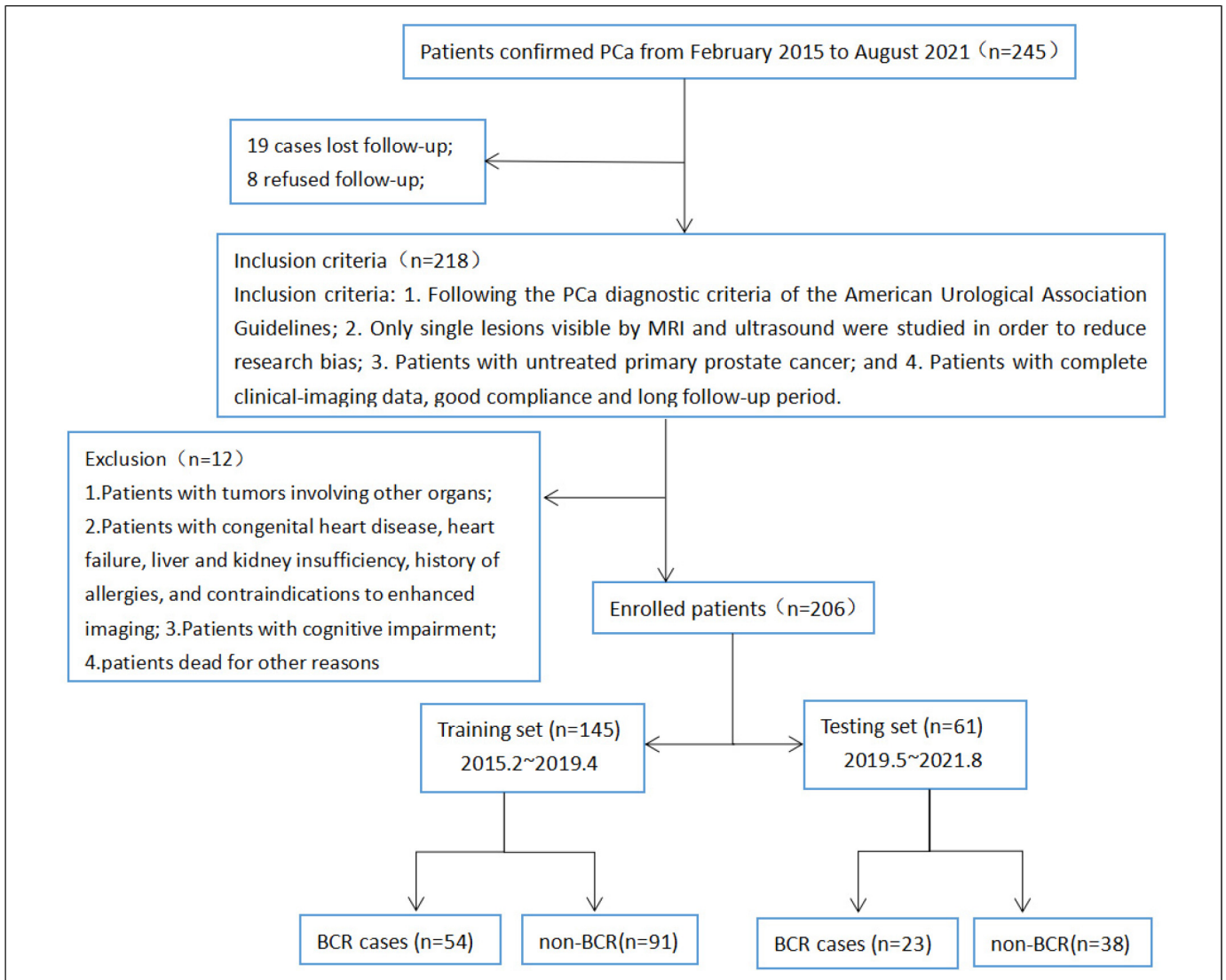This is an exploratory, single-center, and retrospective study. This study was approved by the local Institutional Review Board (Issue No. 1365 [2016]) conducted in accordance with the Declaration of Helsinki. Written informed consent was obtained from individual or guardian participants. The reporting of this study conforms to STROBE guidelines.[12] Our team has de-identified patient details such that the identity of any person may not be ascertained in any way.

Research Method

Baseline clinical data: Age, hypertension, diabetes, and history of smoking and alcohol use; laboratory parameters: BMI, PSA; pathological data: TNM staging and Gleason grade of tumor.

MRI: Philips Achieva 1.5T Nova Dual MRI scanner and GE discovery MR750W 3.0T MRI scanner were used, with appropriate body array coils. The patients took a supine position. The conventional scan sequences included axial, coronal, and sagittal fast spin-echo T2WI of the prostate and seminal vesicles; scan parameters: TR 4700 ms, TE 84 ms, FOV 26×26 cm, matrix 288×224, slice thickness 55 mm, and slice interval 1.0 mm. Axial DWI scan was performed, with b-values of 0 and 800 s/mm^2 and the following scan parameters: slice thickness 3.0 mm, slice interval 1 mm, TR 5250 ms, TE 98.7 ms, FOV 26×26 cm, matrix 128×128. ADC images were obtained on the workstation. PWI scanning: reverse angle 15 degrees, TR 5.08 ms, TE 1.77 ms, single phase scanning duration 8 s, 35 phases in total, and PWI scanning duration 280 s. At the end of the second phase of PWI scanning, the contrast agent Gd DTPA (Gadopentetate Dimeglumine Injection) was
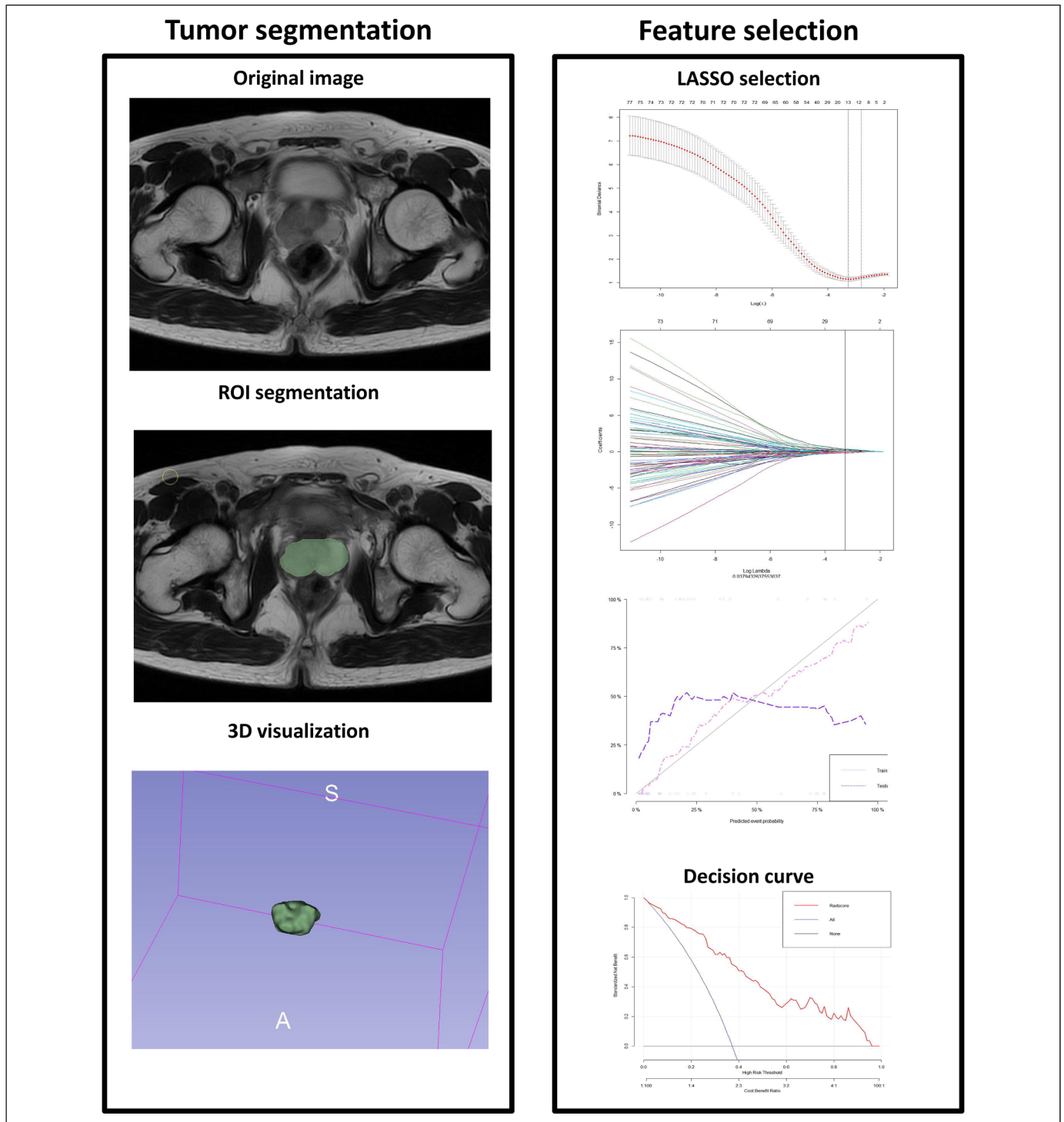
Figure 3. Workflow of radiomics analysis. The left figure shows the outline of the whole prostate and volume of interest; The right figure shows the method and characteristic coefficient convergence diagram of cross-validation with 10 folds in the Least absolute shrinkage and selection operator (LASSO). By adjusting different parameters λ, the binomial deviation of the implementation model is minimal, to screen out the best feature set. Vertical dotted line indicates the best Log(λ) corresponding to the value λ value. The radiomics workflow started with 3-dimensional segmentation of the whole prostate in magnetic resonance perfusion-weighted imaging (MR-PWI) images. After segmentation, radiomic features including shape, intensity, and texture were extracted with or without wavelet filter of the images. LASSO with 10-fold cross validation was used for the radiomic feature selection. Next, radiomics signature was built with the logistic regression model/combined model, and receiver operating characteristic (ROC) curve was plotted.

simultaneously injected via the median cubital vein with a high-pressure syringe at an injection flow rate of 2 mL/s and a dose of 0.2 mmol/kg, and then 20 mL normal saline was injected intravenously at the same flow rate. T2WI, ADC, and PWI images were exported as DICOM files and imported into 3D Slicer for volume of interest (VOI) delineation and feature extraction. VOI delineation was performed manually by 2 experienced radiologists independently, who were blinded to the pathological results. On the

Table 1. Useful Texture Features Filtered From 3 Sequences (T2WI and PWI Sequences) Using LASSO Regression.[a]

T2WI Sequence Features	Coefficients
Ngtdm-Contrast…479	0.01690926
Glcm-ClusterShade…129	0.09519916
Glcm-InverseVariance…514	0.16524954
Glcm-MaximumProbability…705	0.17386981
Ngtdm-ZoneVariance…475	0.23140284
Glszm-SmallAreaLowGrayLevelEmphasis…658	0.25655091
Glrlm-RunVariance…549	0.37085849
Glcm-Imc1…698	0.37147576
Glszm-GrayLevelNonUniformity…88	0.40438271
PWI sequence features	**Coefficients**
Firstorder-90Percentile…110	0.005440154
Firstorder-Median…211	0.010627703
Glcm-Correlation…411	0.085408622
Glszm-LargeAreaHighGrayLevelEmphasis…93	0.105163822
Shape-SurfaceVolumeRatio…12	0.148496187
Glcm-ClusterShade…408	0.153583141
Shape-Flatness…2	0.161620079
Glcm-ClusterShade…129	0.196138213
Glszm-ZoneEntropy…380	0.246620498
Glrlm-RunEntropy…638	0.271043164
Glrlm-RunVariance…735	0.369253021

[a]Scripts have been made available as supplementary information or a web link in the manuscript (https://pan.baidu.com/s/17aXaiI0_f1A2v1CN8PPhxQ?pwd=1234).

T2WI, PWI, and ADC images, VOI was delineated in the maximum axial slice along with the whole prostate margins, keeping away from the urethra, ejaculatory duct, bleeding, and calcified foci. Texture parameters, namely, firstorder, glcm, shape, and ngtdm, were obtained using 3D slicer module (SlicerRadiomics). The agreement between 2 repeated VOIs was assessed by intraclass correlation coefficient (ICC) within observers (ICC≥0.7 indicated a good agreement). For each sequence, 879 features were obtained. These features were introduced into the R software or Python to select valuable texture parameters and generate Radscore by Lasso Regression (Least absolute shrinkage and selection operator) (Figure 3).[13,14]

Ultrasound: Mindray Resona R9 Ultrasound Machine and Philips iU22 ultrasound system were used, along with broadband transrectal convex array transducer (frequency range 4.0-9.0 MHz). The patients received simple enema to clean the bowel. In the left lateral position, the transducer was wrapped in a medical condom or probe sleeve and inserted into the rectum. First, the conventional transrectal prostate ultrasound was performed. The prostate density distribution, blood flow signals, prostate size, and tumor diameter were observed. Sulfur hexafluoride microbubbles (SonoVue®, Bracco) were first diluted with 5 mL of normal saline and shaken well. Bolus injection of 2.4 mL of the dilution of sulfur hexafluoride microbubbles was first performed, followed by rapid bolus of 5 mL of normal saline. Transrectal CEUS of the rectum was performed, and the videos were stored in a hard disc. TIC analysis or QLAB software was used to record the peak intensity (PI), ascending slope (Σ), time to peak (TTP), arrival time (AT), and area under the curve (AUC) of the time-intensity curve. All examinations were performed by 2 associate chief physicians at the ultrasound department independently. Any divergence of opinion was settled by inviting a third party, a sonographer with senior title. Final reports were issued after reaching an agreement.[15,16]

Radical surgery and follow-up for PCa: The patients received general anesthesia. Dissociation was performed in the retrorectal space to expose the prostate apex, prevesical

Table 2. Logistic Regression Analysis Results of General Clinical Model Based on Clinical Features for Predicting the BCR.

General clinical model Factors	Univariate analysis		Multivariate analysis	
	P	Hazard ratio	*P*	Hazard ratio
Hypertension	.69	0.99 (0.97-1.02)		
Diabetes	.86	1.01 (0.97-1.03)		
History of smoking	.14	1.01 (0.99-1.03)		
History of alcohol use	.06	0.98 (0.96-1.00)		
Age	.68	0.99 (0.96-1.02)		
Prostate volume	.09	0.98 (0.96-1.00)		
Tumor diameter	<.05[a]	1.26 (1.09-1.46)	.03[a]	1.18 (1.01-1.39)
BMI	.41	0.97 (0.90-1.04)		
Clinical TNM stage	.01[a]	1.85 (1.12-3.07)		
Lymph node metastasis	.01[a]	1.26 (1.04-1.53)	.03[a]	1.29 (1.02-1.63)
Distant metastasis	.01[a]	2.09 (1.17-3.71)		
GleasonSum	<.05[a]	1.30 (1.13-1.50)	.00[a]	1.32 (1.13-1.55)
Preoperative PSA	.02[a]	1.05 (1.01-1.10)	<.05[a]	1.08 (1.02-1.13)
Treatment mode	.75	1.03 (0.84-1.26)		

Abbreviations: BMI, body mass index; BCR, biochemical recurrence; TNM, tumor node metastasis classification.
[a]$P < .05$.

space, and etropubic space. The bladder neck was reconstructed after prostate resection, followed by urethral anastomosis. The resected PCa tissues were subjected to pathological examination and Gleason grading. The PSA level was determined regularly after surgery. In the first 2 years, the PSA level was determined one month after surgery and then once every 3 months, along with other follow-up procedures. The PSA level was determined once every 6 months 2 years later. MRI was performed if necessary, during the follow-up. Patients with 2 or more elevations of the PSA level ($\geq$0.2 ng/mL) were included in the study group, while the remaining were included in the control group.[17,18]

Statistics

All statistical analyses were conducted using SPSS 22.0. If the data passed the normality test, they were expressed as X$\pm$s and compared by t test; otherwise, the intergroup comparisons were conducted using the Mann-Whitney U test. When $P <$ .05, the finding was considered statistically significant. More informative radiomics features were selected, and Radscore was generated using Lasso Regression. A 10-fold cross-validation was used for calculating the radiomics performance on the features extraction. The models based on the patients' general clinical data, CEUS, and MRI radiomics and the combined model were built using logistic regression, respectively. The predictive value of each model was analyzed by plotting ROC curves. $P <$ .05 indicated a significant difference. The higher the AUC, the greater the predictive efficacy would be. The decision curves and the nomographs were generated using the R software (the R Project for Statistical Computing, version 3.4.1).[19,20]

Result

1. At the end of the follow-up, 19 out of 245 PCa patients were lost to the follow-up; 8 patients refused to attend the follow-up; 8 patients were combined with other carcinomas or liver and kidney dysfunction; 4 patients with cognitive dysfunction; 77 patients with PCa were included into the BCR group; and 129 patients with PCa but no BCR were included into the normal group. According to our follow-up, the incidence of BCR 1 to 7 years (median follow-up time for BCR and No-BCR patients were 3.8/

Table 3. Logistic Regression Analysis Results of CEUS Model Based on CEUS Features for Predicting the BCR.

CEUS model	Univariate analysis		Multivariate analysis	
Factors	P	Hazard ratio	P	Hazard ratio
PI	.03[a]	1.05 (1.00-1.10)		
Σ	.69	1.97 (0.06-59.46)		
TTP	.27	0.98 (0.95-1.01)		
AT	<.05[a]	1.07 (1.02-1.13)	<.05[a]	1.08 (1.02-1.14)
AUC	.15	0.98 (0.95-1.01)		
Elastography grade	.04[a]	1.19 (1.01-1.41)		

Abbreviations: PI, peak intensity; Σ, ascending slope; TTP, time to peak; AT, arrival time; AUC, area under the curve; CEUS, contrast-enhanced ultrasound; BCR, biochemical recurrence.
[a]$P <$ .05.

Table 4. Logistic Regression Analysis Results of MRI-Radiomics Model Based on Radiomics Features for Predicting the BCR.

MRI-radiomics model	Univariate analysis		Multivariate analysis	
	P	Hazard ratio	P	Hazard ratio
Radscore1	<.05[a]	3.43 (1.91-6.16)	<.05[a]	3.25 (1.65-6.39)
Radscore2	<.05[a]	2.63 (1.93-3.58)	<.05[a]	2.60 (1.89-3.57)
Radscore3	>.05	/		

Abbreviations: BCR, biochemical recurrence; MRI, magnetic resonance imaging.
[a]$P <$ .05.

Table 5. Logistic Regression Analysis Results of Combined Model Based on CEUS-MRI-Clinical Features for Predicting the BCR.

Combined model	Univariate analysis		Multivariate analysis	
Factors	P	Hazard ratio	P	Hazard ratio
Tumor diameter	<.05[a]	1.26 (1.09-1.46)		
Clinical TNM stage	.01[a]	1.85 (1.12-3.07)		
Lymph node metastasis	.01[a]	1.26 (1.04-1.53)		
Distant metastasis	.01[a]	2.09 (1.17-3.71)		
GleasonSum	<.05[a]	1.30 (1.13-1.50)	.04[a]	1.24 (1.01-1.54)
Preoperative PSA	.02[a]	1.05 (1.01-1.10)	.04[a]	1.07 (1.00-1.14)
PI	.03[a]	1.05 (1.00-1.10)		
AT	<.05[a]	1.07 (1.02-1.13)	.03[a]	1.09 (1.01-1.19)
elastography grade	.04[a]	1.19 (1.01-1.41)		
Radscore1	<.05[a]	3.43 (1.91-6.16)	<.05[a]	5.28 (1.85-9.89)
Radscore2	<.05[a]	2.63 (1.93-3.58)	<.05[a]	2.60 (1.81-3.73)

Abbreviations: CEUS, contrast-enhanced ultrasound; BCR, biochemical recurrence; PI, peak intensity; AT, arrival time; MRI, magnetic resonance imaging; TNM, tumor node metastasis classification.
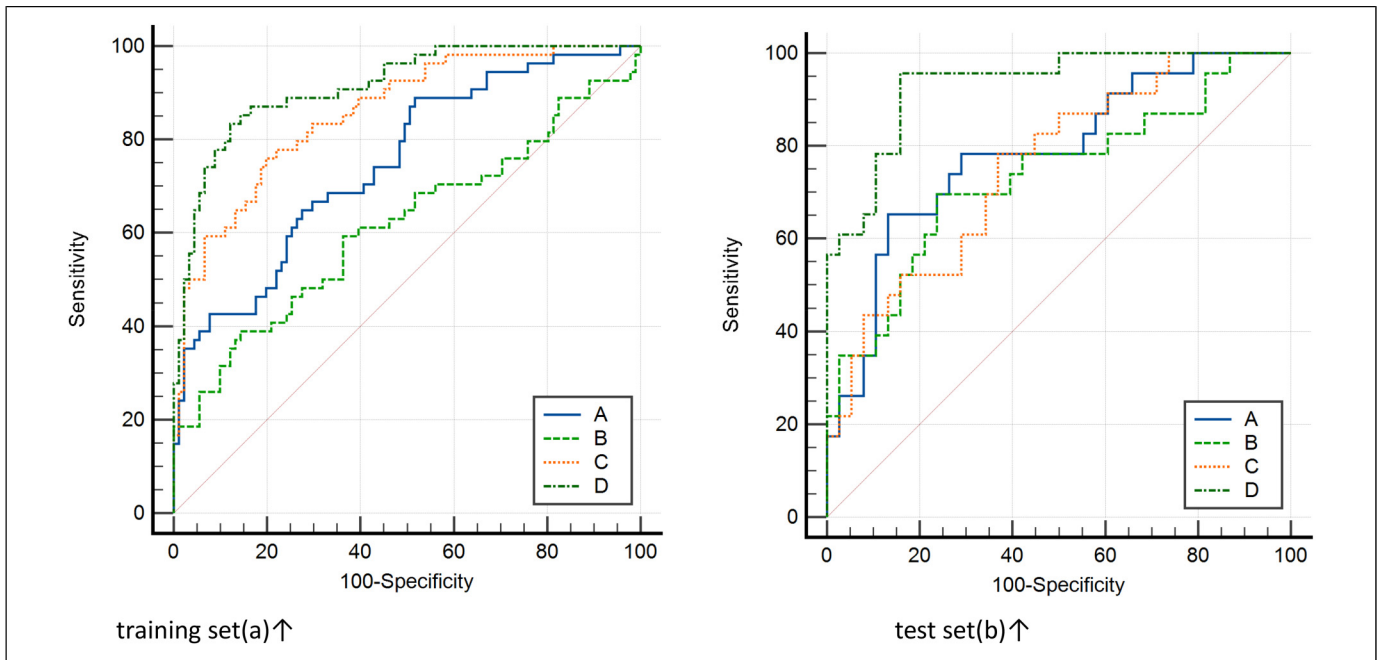[a]$P <$ .05.

Figure 4. Delong test method was used to compare the area under the curve of ROC between different prediction models of training set (left) and test set (right) and compare its effectiveness in predicting the biochemical recurrence (BCR). The area under the curve of the combined model was the largest.[19] *Notes:* The clinical model (A), contrast-enhanced ultrasound (CEUS) model (B), magnetic resonance imaging (MRI) radiomics model (C), and combined model (D). training set(a)↑ test set(b)↑.
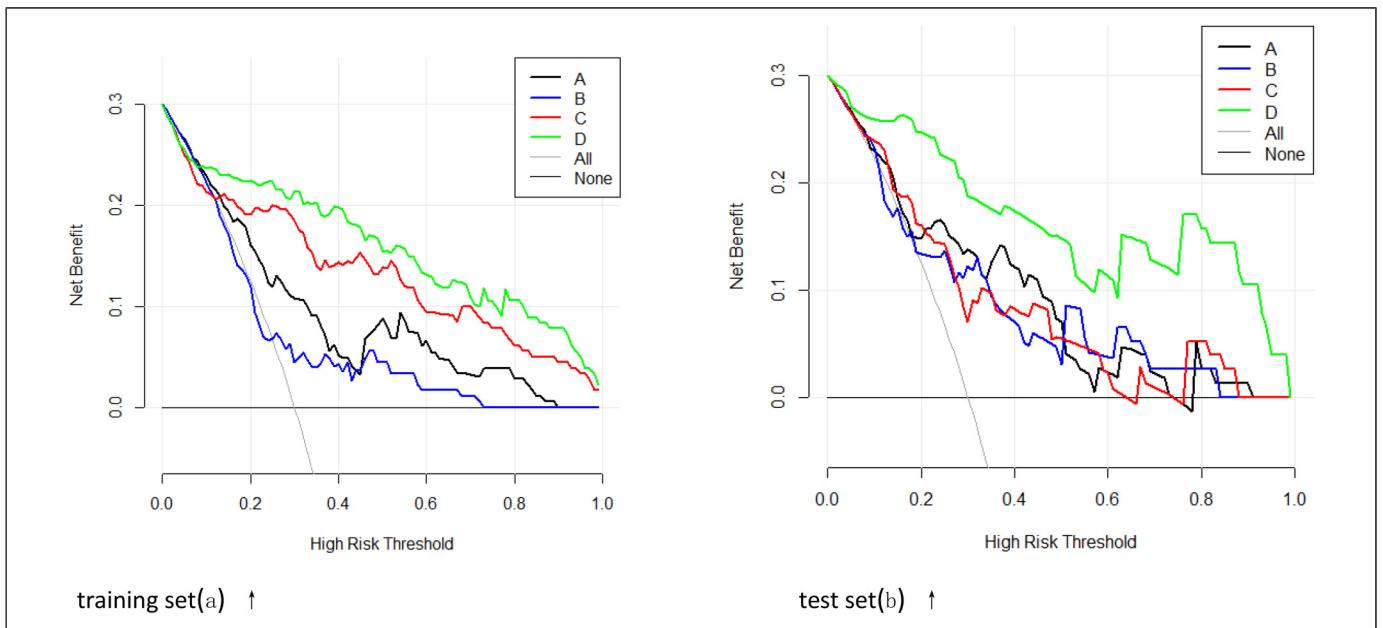

Figure 5. In the training set (left) and the test set (right), the prediction performance and net benefit of the clinical model (A), contrast-enhanced ultrasound (CEUS) model (B), magnetic resonance imaging (MRI) radiomics model (C), and combined model (D) are compared using the decision curve analysis, it is confirmed that the combined model had the highest net benefit. training set(a) ↑ test set(b) ↑.

5.1 years, respectively) after surgery was 37.38% in 206 PCa patients at XX hospital based on clinical and radiographic findings.

2. We ran the 3D Slicer software for VOI delineation, which resulted in 879×3 groups of texture data. After removing 29×3 groups of invalid texture parameters by ICC test, the
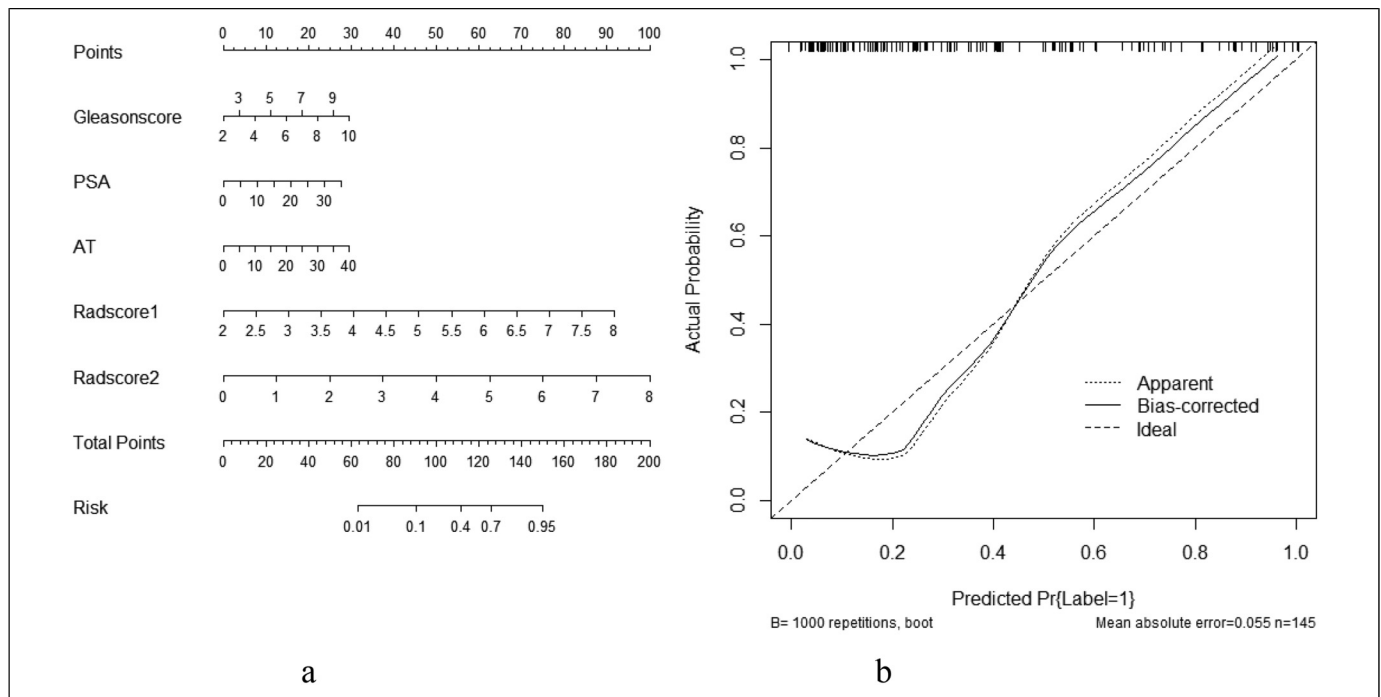
Figure 6. The nomogram prediction tool based on the risk factors of the combined model was used clinically (a. nomogram, b. Calibration curve).

consistency correlation coefficients of the remaining 850×3 radiomics features extracted within and between groups in this study are 0.750 to 0.998 and 0.751 to 0.999, respectively, with the average coefficients of 0.889 and 0.888; This shows that the 3D-ROI manually segmented layer by layer in this study has high consistency and stability, so all 850×3 radiomics feature parameters extracted are included in the subsequent feature screening. Through the Lasso Regression, we obtained 3 groups of Radscore (Radscore 1/2/3 corresponded to T2WI, PWI, and ADC sequences, respectively) (Table 1). Both groups' ADC features screening results are invalid using LASSO regression and so are not displayed in Table 1.

The specific meanings of some texture parameters are as follows:

Histogram features: Including firstorder, shape, gray mean, maximum, minimum, variance, and percentile.

Texture features:

Absolute Gradient reflects the degree or suddenness of gray intensity fluctuation in an image. For 2 adjacent pixels or voxels, if one is black and the other is white, the gradient is the highest; if both pixels are black (or both are white), the gradient at this location is zero.

Gray Level Co occurrence Matrix reflects the predefined distance between pixels or voxels in different directions (horizontal, vertical, or diagonal of 2D analysis or 13 directions of 3D analysis) and captures the spatial relationship of pixel pairs or voxel pairs with predefined gray intensity.

The Gray Level Run Length Matrix (GLRLM) provides information about the 2-dimensional or 3-dimensional spatial distribution of consecutive pixels of the same gray level in one or more directions.

The Gray Level Size Zone Matrix (GLSZM for short) is like GLRLM in principle, but the more uniform texture of GLSZM will lead to a wider and flatter matrix, which is helpful for the weight calculation of the system.

The Neighboring Gray Tone Difference Matrix quantifies the sum of differences between the gray level of a pixel or voxel and the average gray level of its adjacent pixels or voxels within a predefined distance.

The Gray Level Dependence Matrix reflects the gray level similarity and gray level dependency in the entire ROI.

3. The univariate analysis to identify the influence factors of BCR following the surgery for PCa: The 2 groups of patients differed significantly in the Tumor diameter, TNM stage of tumor, lymph node metastasis or distance metastasis, Gleason grade, preoperative PSA, ultrasound (PI, AT, elastography grade), and MRI-radscore1/2 ($P < .05$) (Tables 2-4). *Multivariate analysis:* GleasonSum, preoperative PSA, AT, and Radscore1/2 were independent risk factors for BCR ($P < .05$) (Table 5).

4. Building several predictive models and external validation

Four predictive models (general clinical model included tumor diameter, clinical TNM stage, lymph node metastasis, distant metastasis, GleasonSum, Preoperative PSA; CEUS model included PI, AT, elastography grade; MRI radiomics model included Radscore1, Radscore2; and combined model included all above;) were built based on the above risk factors in the training set. The predictive efficacy of the 4 models was compared using the MedCalc Software. It was found that the combined model had the highest predictive value (AUC: 0.91; odds ratio [OR] 0.02, 95% confidence interval [CI]: 0.85-0.95). The difference was statistically significant compared with the model based on general clinical data (AUC: 0.74; OR 0.04,

95% CI: 0.67-0.81, P < .05), CEUS (AUC: 0.61; OR 0.05, 95% CI: 0.53-0.69, P < .05), and MRI radiomics (AUC: 0.85; OR 0.03, 95% CI: 0.78-0.91, P = .01). The decision curve analysis (DCA) also confirmed the higher net benefit of the combination model. The external validation on the testing set yielded the same result: The combined model (AUC: 0.93; OR 0.03, 95% CI: 0.83-0.98) outperformed the model based on general clinical data (AUC: 0.78; OR 0.06, 95% CI: 0.66-0.87, P < .05), CEUS (AUC: 0.73; OR 0.07, 95% CI: 0.60-0.83, P = .01), and the model based on MRI radiomics (AUC: 0.75; OR 0.06, 95% CI: 0.62-0.85, P < .05). The nomogram generator tool and the calibration curves developed using the R software had been used in clinical settings (Figures 4-6).

Discussion

According to WHO statistics, over 1.4 million males are confirmed with PCa in European and American regions every year according to World Cancer Report 2021 (WHO). About 50% of PCa patients will receive radical prostatectomy and 20% to 30% of them are combined with BCR.[1,2,20] In recent years, China has witnessed a growing incidence of PCa, and about 30% of BCR patients are faced with the risk of death.[2,4] BCR initially presents with a postoperative elevation of the PSA level but no specific clinical or radiographic metastases. BCR indicates the presence of residual prostate epithelial cells in PCa patients. Besides, the clinical course of disease varies dramatically from one patient to another. About 50% of BCR patients experience rapid clinical deterioration before the metastasis; about 30% of BCR patients are combined with a fluctuating PSA level and achieve long-term survival due to drug-induced immune activation though the life expectancy decreases. Very few patients are observed to be not adversely affected in terms of life quality. Therefore, predicting PCa-BCR can inform potential adjustment of the therapeutic regimen, thereby improving the patients' life quality. Studies have confirmed that early prediction and intervention of PCa-BCR can dramatically arrest or reduce metastases.[14,21] In the present study, we selected reliable MRI radiomics features using the lasso regression. A combination model integrating patients' clinical information, CEUS, and MRI-based radiomics features was built for noninvasive prediction of BCR. This model can dramatically reduce patients' economic burden and has a proven predictive efficacy in PCa patients.[21,22]

Our search of PubMed and Scopus databases produced very few reports on PCa-BCR prediction that combined ultrasound and MRI (less than 10). Moreover, no articles involving the use of MR PWI-based radiomics have been published yet.[16,17] The incidence of BCR in 1 to 7 years postoperative was 37.38% in PCa patients in this study. This incidence was slightly higher than what has been reported earlier, which might be explained by population variation, limited sample size, and longer follow-up duration. Given the above, postoperative long-term follow-up for prognostic monitoring of PCa and developing early predictive tool for PCa-BCR are highly important.[23] To extract more predictive features for PCa-BCR, we compared the clinical and radiographic features selected by Lasso Regression between the 2 groups. The univariate analysis showed that Tumor diameter, TNM stage of tumor, lymph node metastasis or distance metastasis, Gleason grade, preoperative PSA, ultrasound (PI, AT, and elastography grade), and MRI-radscore1/2 were statistically significant features (P < .05). The multivariate regression analysis confirmed that the GleasonSum, preoperative PSA, AT, and Radscore1/2 were independent risk factors for PCa-BCR. The above results indicated that tumor diameter, TNM stage, and ultrasound feature (PI and elastography grade) jointly poorly predicted the prognosis of PCa-BCR. The therapeutic method and TNM stage have been established as important indicators for PCa-BCR in recent years' studies.[6,11] However, we found a weak efficacy of both as an independent predictor in this study. Neither could it be used to predict PCa-BCR in a fraction of patients with substantial individual difference. This finding may be attributed to the unique evolutionary course of the disease in individual differences cases. This study confirmed that the GleasonSum is still a reliable parameter for predicting BCR because the histological score provides the differentiation grade of prostate cancer and the intrinsic nature of tumor. Preoperative PSA is a commonly used biochemical parameter in the department of urologic surgery. However, we reported a poor specificity of preoperative PSA level and its susceptibility to the influence of reagent sensitivity and potential diseases (urinary tract infection, prostatitis, and prostatic hyperplasia). PSA alone usually has a low predictive accuracy (0.613) for PCa-BCR.[23–25] Therefore, it is more effective to use these 2 indicators as joint indicators for the clinical management of BCR.

Among various ultrasound indicators, AT may become an effective parameter for predicting PCa-BCR, given the abundant blood supply and low degree of differentiation of tumor in patients with PCa-BCR.[17] Radiomics, first introduced by Lambin *et al* from Belgium in 2012, was initially used in CT-based diagnosis.[26] This technique has been successfully developed and applied to clinical studies along with the progress in computer vision coupled to 3D Slicer and ITK-snap software. At present, machine learning algorithms in the general sense have been applied to medical research in a wide array of sectors, improving diagnostic and therapeutic efficacy. Gnanapragasam *et al* built the predictive model for PCa based on the ensemble algorithm, achieving an accuracy of >75%. Clarke *et al* built the predictive model for PCa based on convolutional neural network, logistic regression analysis, and random forest algorithm, achieving an accuracy of >80%.[24,27,28] To predict PCa-BCR, we introduced the lasso logistic regression-based radiomics, which achieved a good benefit. We delineated MRI-VOI preoperatively in 206 PCa cases before surgery and implemented the screening procedure. Three groups of reliable Radscore data were generated to represent the integrated texture differences across the lesions, ensuring high heterogeneity and reducing biases.[26–28] Four predictive models were built based on the above risk factors using the training set. The predictive performance of the combined model was proven by external validation on the validation/test set. This finding was further

supported by the DCA. The nomogram thus drawn simplified the prediction workflow for PCa-BCR. The nomogram was an integration of the patients' clinical, CEUS, and radiographic information, offering parameter values that fully account for individual differences of PCa patients. Hence, the predictive accuracy of the combination model was improved, as has been demonstrated in clinical settings. In addition, compared with previous clinical models and radiomics machine learning models, this research model has many advantages. First of all, the combined model integrates clinical data, CEUS parameters, and MRI radiomics parameters, which can well mine clinical image data, reduce bias, and better reflect the population differences of BCR; In addition, the nomogram developed by the model is simple and practical, which provides support for clinical decision making of BCR in later stage. More importantly, we found that MR-PWI is of great value in prostate cancer diagnosis and BCR prediction. Because the typical enhancement mode of highly malignant tumors is typical and extreme "fast in and fast out or Ultimate slope," the texture parameters extracted by PWI multistage enhancement and contrast mode will certainly improve the prediction performance of the model, which is widely confirmed.[28,29]

Limitations

(1) Since this was a single-center study with small sample size, we didn't calculate sample size using random sampling, whole group sampling, or other statistical methods; The number of cases included in the present study was small. The findings should be enriched by more multicenter studies in the future; (2) Artificial intelligence and deep learning techniques were not used for radiomics feature extraction; (3) Pathomics or Ultrasonomics was not considered for the study, resulting in insufficiency of mining of ultrasound-pathological data; and (4) The robustness of MRI-based radiomic features was not examined using the data from other facilities. Because this study used Radscore for prediction (ie, many predictive features were used for model building), generalizability of this model might be limited.[29,30]

Conclusion

To conclude, the predictive model for PCa-BCR based on clinical features, CEUS features, and MR-PWI radiomics features offers a new pathway for PCa-BCR prediction, which may further improve the clinical decision-making and postoperative survival of PCa patients.

Authors' Note

The experimental protocol was established, according to the ethical guidelines of the Helsinki Declaration, and was approved by the Human Ethics Committee of Xiangyang No. 1 People's Hospital (Issue No. 1365 [2016]). Written informed consent was obtained from individual or guardian participants. All data generated or analyzed during this study are included in this published article, or contact the email address of the corresponding author and ask for it.

Authors' Contribution

PA, PQ, YL, GF, and YH conceived and drafted the manuscript. WG and XL contributed to the literature review and are responsible for collecting and collating clinical data. YJY, YH, and YL revised the manuscript critically for important intellectual content. XL, GF, and YL are responsible for the quality control of article statistics. GF and PS approved the final version to be published and agreed to act as guarantors of the work. PA, YL, and YH contributed equally to this work.

Declaration of Conflicting Interests

The author(s) declared no potential conflicts of interest with respect to the research, authorship, and/or publication of this article.

ORCID iDs

Peng An https://orcid.org/0000-0002-0048-2738
YingJian Ye https://orcid.org/0000-0001-6220-0866
Ping Song https://orcid.org/0000-0002-8131-6343

References

1. Culp MB, Soerjomataram I, Efstathiou JA, Bray F, Jemal A. Recent global patterns in prostate carcinoma incidence and mortality rates. *Eur Urol*. 2020;77(1):38-52.
2. Siegel DA, O'Neil ME, Richards TB, Dowling NF, Weir HK. Prostate carcinoma incidence and survival, by stage and race/ethnicity—United States, 2001–2017. *MMWR Morb Mortal Wkly Rep*. 2020;69(41):1473-1480. Published 2020 Oct 16.
3. Gandaglia G, Leni R, Bray F, et al. Epidemiology and prevention of prostate carcinoma. *Eur Urol Oncol*. 2021;4(6):877-892.
4. Zhu Y, Mo M, Wei Y, et al. Epidemiology and genomics of prostate carcinoma in Asian men. *Nat Rev Urol*. 2021;18(5):282-301.
5. Kimura T, Egawa S. Epidemiology of prostate carcinoma in Asian countries. *Int J Urol*. 2018;25(6):524-531.
6. Murata Y, Tatsugami K, Yoshikawa M, et al. Predictive factors of biochemical recurrence after radical prostatectomy for high-risk prostate carcinoma. *Int J Urol*. 2018;25(3):284-289.
7. Harnden P, Shelley MD, Naylor B et al. Does the extent of carcinoma in prostatic biopsies predict prostate-specific antigen recurrence? A systematic review. *Eur Urol*. 2008;54(4):728-739.
8. Zhang X, An P, Ye YJ, et al. Minimally invasive surgery group of Chinese anti carcinoma association genitourinary oncology committee. *Zhonghua Wai Ke Za Zhi*. 2017;55(10):721-724.

9. Cookson MS, Aus G, Burnett AL, et al. Variation in the definition of biochemical recurrence in patients treated for localized prostate cancer: the American Urological Association Prostate Guidelines for localized prostate cancer update panel report and recommendations for a standard in the reporting of surgical outcomes. *J Urol.* 2007;177(2):540-545.

10. Zaorsky NG, Calais J, Fanti S, et al. Salvage therapy for prostate cancer after radical prostatectomy. *Nat Rev Urol.* 2021;18(11):643-668.

11. Sanda MG, Cadeddu JA, Kirkby E, et al. Clinically localized prostate cancer: AUA/ASTRO/SUO guideline. Part I: risk stratification, shared decision making, and care options. *J Urol.* 2018;199(3):683-690.

12. von Elm E, Altman DG, Egger M, et al. The strengthening the reporting of observational studies in epidemiology (STROBE) statement: guidelines for reporting observational studies. *Ann Intern Med.* 2007;147(8):573-577.

13. Ploussard G, Renard-Penna R. MRI-guided active surveillance in prostate carcinoma: not yet ready for practice. *Nat Rev Urol.* 2021;18(2):77-78.

14. Turkbey B, Choyke PL. Multiparametric MRI and prostate carcinoma diagnosis and risk stratification. *Curr Opin Urol.* 2012;22(4):310-315.

15. Kanagaraju V, Ashlyin PVK, Elango N, Devanand B. Role of transrectal ultrasound elastography in the diagnosis of prostate carcinoma. *J Med Ultrasound.* 2020;28(3):173-178.

16. Correas JM, Halpern EJ, Barr RG, et al. Advanced ultrasound in the diagnosis of prostate carcinoma. *World J Urol.* 2021;39(3):661-676.

17. Mannaerts CK, Wildeboer RR, Remmers S, et al. Multiparametric ultrasound for prostate carcinoma detection and localization: correlation of B-mode, shear wave elastography and contrast enhanced ultrasound with radical prostatectomy specimens. *J Urol.* 2019;202(6):1166-1173.

18. Heidenreich A, Bastian PJ, Bellmunt J, et al. EAU guidelines on prostate cancer. Part II: Treatment of advanced, relapsing, and castration-resistant prostate cancer. *Eur Urol.* 2014;65(2):467-479.

19. DeLong ER, DeLong DM, Clarke-Pearson DL. Comparing the areas under two or more correlated receiver operating characteristic curves: a nonparametric approach. *Biometrics.* 1988;44(3):837-845.

20. Vickers AJ, Elkin EB. Decision curve analysis: a novel method for evaluating prediction models. *Med Decis Making.* 2006;26(6):565-574.

21. Prezioso D, Iacono F, Romeo G, Ruffo A, Russo N, Illiano E. Early versus delayed hormonal treatment in locally advanced or asymptomatic metastatic prostatic carcinoma patient dilemma. *World J Urol.* 2014;32(3):661-667.

22. Luo Y, Gou X, Huang P, Mou C. Prostate carcinoma antigen 3 test for prostate biopsy decision: a systematic review and meta analysis. *Chin Med J (Engl).* 2014;127(9):1768-1774.

23. Ahlering TE, My Huynh L, Towe M, et al. Testosterone replacement therapy reduces biochemical recurrence after radical prostatectomy. *BJU Int.* 2020;126(1):91-96.

24. Cuocolo R, Cipullo MB, Stanzione A, et al. Machine learning applications in prostate carcinoma magnetic resonance imaging. *Eur Radiol Exp.* 2019;3(1):35. Published 2019 Aug 7.

25. Suarez-Ibarrola R, Hein S, Reis G, Gratzke C, Miernik A. Current and future applications of machine and deep learning in urology: a review of the literature on urolithiasis, renal cell carcinoma, and bladder and prostate carcinoma. *World J Urol.* 2020;38(10):2329-2347.

26. Smith CP, Czarniecki M, Mehralivand S, et al. Radiomics and radiogenomics of prostate carcinoma. *Abdom Radiol (NY).* 2019;44(6):2021-2029.

27. Lee C, Light A, Alaa A, Thurtle D, van der Schaar M, Gnanapragasam VJ. Application of a novel machine learning framework for predicting non-metastatic prostate carcinoma-specific mortality in men using the Surveillance, Epidemiology, and End results (SEER) database. *Lancet Digit Health.* 2021;3(3):e158-e165. Epub 2021 Feb 3. PMID: 33549512.

28. Michallek F, Huisman H, Hamm B, et al. Prediction of prostate cancer grade using fractal analysis of perfusion MRI: retrospective proof-of-principle study. *Eur Radiol.* 2022;32(5):3236-3247.

29. Saito T, Yamasaki F, Kajiwara Y, et al. Role of perfusion-weighted imaging at 3T in the histopathological differentiation between astrocytic and oligodendroglial tumors. *Eur J Radiol.* 2012;81(8):1863-1869. Epub 2011 May 4. PMID: 21543173.

30. Kutluhan MA, Ünal S, Özsoy E, et al. Evaluation of four preoperative models for prediction of biochemical recurrence after radical prostatectomy in localised prostate carcinoma. *Int J Clin Pract.* 2021;75(10):e14682.